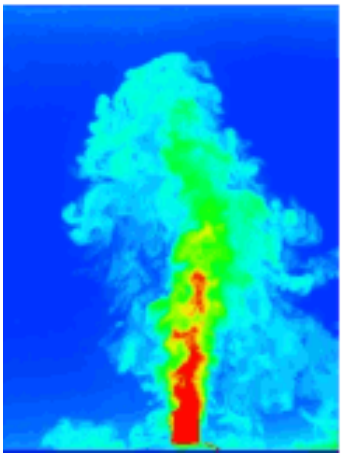

Journal of Turbulence
Publication details, including instructions for authors and subscription information:
http://www.informaworld.com/smpp/title~content=t713665472

On the phase velocities of the motions in an offset attaching planar jet

N. Gao[1] [a]; D. Ewing[2] [a]
[a] Department of Mechanical Engineering, McMaster University, Hamilton, Ontario, Canada

First Published on: 01 January 2008

To cite this Article Gao[1], N. and Ewing[2], D.(2008)'On the phase velocities of the motions in an offset attaching planar jet',Journal of Turbulence, Volume 9, Art. No. N27,

To link to this Article: DOI: 10.1080/14685240802301965

URL: http://dx.doi.org/10.1080/14685240802301965

Journal of Turbulence
Vol. 9, No. 27, 2008, 1–21

Taylor & Francis
Taylor & Francis Group

On the phase velocities of the motions in an offset attaching planar jet

N. Gao[1*] and D. Ewing[2]

Department of Mechanical Engineering, McMaster University, Hamilton, Ontario, Canada L8S 4L7

(*Received 3 December 2007; final version received 24 June 2008*)

An experimental investigation was performed to characterize the phase velocity of different frequency fluctuations in a turbulent offset attaching jet with a Reynolds number of 44 000 and initial offset distance of H_j. The velocities were determined from the change in the phase of the cross-spectra of the fluctuating pressure along the wall and the cross-spectra of the fluctuating wall pressure and fluctuating velocity throughout the flow. The results showed there was upstream propagation of the wall pressure fluctuations near the separation point associated with the flapping motion, but the upstream propagation apparent in the correlation coefficient of the pressure was due to higher frequency fluctuations associated with the recirculating flow. The phase velocities determined from the pressure–velocity cross-spectra for the higher frequency motions showed less-frequency dependence and less acceleration than those determined from the pressure cross-spectra. There was also evidence of two velocities for the shear layer motions and a velocity for the lower frequency wall jet motions not apparent in the results from the pressure cross-spectra. Thus, the phase velocities determined from pressure cross-spectra do not fully reflect the velocities of the motions in the flow.

Keywords: offset attaching jet; structures; phase velocity; coherence

1. Introduction

There is considerable interest in the dynamics of the pressure fluctuations below separated and reattaching shear layer flows because the pressure fluctuations are important in flow-induced vibrations or noise applications and because there is interest in using the fluctuating pressure as an input to control separated flows. Offset jets with modest offset distances, similar to those consider here, are often used in blown-film manufacturing to cool pliable plastic surfaces that do undergo flow-induced vibrations. Thus, characterizing the nature of the pressure fluctuations induced by the offset jets is important in predicting the onset and nature of these vibrations. The large-scale structures initially interacting with the surface in these offset jets are associated with the attaching inner shear layer [1]. The pressure fluctuations on the wall in this region had many features in common with the fluctuations below other reattaching shear layer flows [2–17], including evidence of a shedding instability with a frequency of $fX_r/U_j \approx 0.5$ to 1 and a low-frequency flapping instability with $fX_r/U_j < 0.2$ [1]. The dominant structures in the offset jets change as the flow

[1] *Current address*: School of Engineering, Sun Yat-sen University, 510275 Guangzhou, People's Republic of China.
[2] *Current address*: Department of Mechanical and Materials Engineering, Queen's University, Kingston, Ontario, Canada.
*Corresponding author. Email: gaonan@mail.sysu.edu.cn

ISSN: 1468-5248 online only

DOI: 10.1080/14685240802301965
http://www.tandf.co.uk/journals

evolves downstream to lower-frequency motions similar to those observed in the planar wall jet [1].

The propagation velocity of the wall pressure fluctuations below attaching flows is often estimated from the time delay to the maximum in the correlation coefficient of the pressure along the wall. The propagation velocity of the pressure fluctuations associated with the shear layer structures below the offset jet determined using this approach increased from $0.5U_j$ near the reattachment point to approximately $0.65U_j$ at $x/X_r \approx 2$ [1] similar to other reattaching shear layer flows [7]. The measurements in the offset jets also showed evidence of upstream propagation near the separation point [1] observed previously in other reattaching flows and thought to be associated with the low-frequency flapping instability [7, 8]. The propagation velocity decreased abruptly in the wall jet region as the fluctuations associated with the wall jet structures became the dominant motions.

Measurements of the correlation coefficient between the fluctuating wall pressure and the fluctuating velocity in the offset jet showed though that the transition from the shear layer motions to the wall jet motions occurred gradually over an extended distance after the jet attached to the wall. The correlation coefficient of the pressure could only yield a single propagation velocity at each location and hence the sudden change in this value when the wall jet structures became dominant near the wall. Both the shear layer and wall jet motions, however, make significant contributions to the fluctuating pressure at different frequencies so it should be possible to deduce both velocities in the transition region from the phase of the fluctuating pressure cross-spectra (or phase velocities) following [8]. Hudy et al. [8] examined the phase velocities for the pressure fluctuations at selected frequencies in the flow over a fence by considering the change in the phase of the pressure cross-spectra with the separation distance along the wall. They found that the phase speed of these motions varied with frequency, though the cause was not clear. There was also evidence of upstream propagation at the frequency associated with the flapping mode, though the phase velocity for other frequencies in this range were not considered. A similar approach could also be applied to simultaneous measurements of the fluctuating wall pressure and the fluctuating velocity at different downstream points in the flow to examine the phase velocity of the velocity fluctuations in the flow field. The relationship between the fluctuating wall pressure and fluctuating velocity has been examined in attaching flows [1, 10, 18]. Heretofore, however, there does not appear to have been a comprehensive investigation of the relationship between the pressure and velocity at different frequencies. Nor does it appear that these measurements have been used to examine the phase velocity of the different frequency velocity fluctuations in the flow.

The objective of this investigation was to examine the dynamics of the wall pressure fluctuations at different frequencies below a reattaching offset jet, and the relationship between the pressure fluctuations on the wall and velocity fluctuations in the flow at different frequencies. The measurements were performed using an array of microphones mounted in the wall and a hot-wire traversed through a jet initially offset one jet height above the wall with a Reynolds number of 44 000. The experimental facility and methodology used in this investigation are outlined in the following section. The measurement results are then presented and discussed. Finally, the conclusions from the study are presented.

2. Experimental methodology

The development of the offset jet was examined for a jet exiting a channel with a height (H_j) of 3.8 cm and a length of 81 cm or $22H_j$ also used in [1]. The width of the channel and the facility (W) was 74.3 cm or 19.5 H_j. The flow into the channel was supplied by a variable speed blower that entered a settling chamber (122 cm × 72.4 cm × 45.7 cm) through five 10 cm diameter hoses.

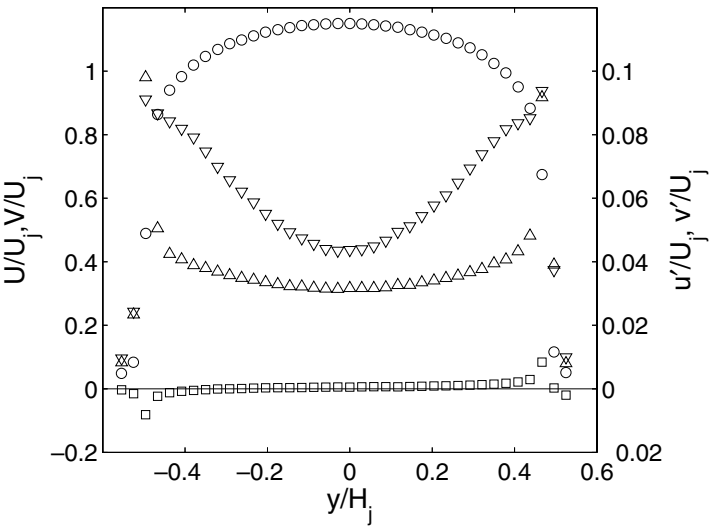

Figure 1. Distribution of the ○ streamwise and □ vertical mean velocities and the △ streamwise and ∇ vertical fluctuating velocities measured at $x/H_j = 0.05$ and $Re \approx 44\,000$ for the jet as a free jet.

The flow was conditioned in the settling chamber using flow straightening sections and screens before entering the channel through a square-edged reentrant entrance. The measurements in this investigation were performed for an average outlet velocity (U_j) of 18.4 m/s that corresponded to a Reynolds number based on jet height of approximately 44 000. The profiles of the mean velocity and fluctuating velocities measured at the jet exit shown in Figure 1 were symmetric and fully developed.

The flow exiting the channel developed over a 180 cm long plate mounted parallel to the channel at a distance (H_s) of 3.8 cm (or H_j) below the bottom of the channel. The flow developed between 100 cm high side walls. The boundary layers on these side walls grew to approximately $5H_j$ at $x/H_j = 12$. The profiles were uniform over the remainder of the jet. Measurements also showed that the lateral integral length scale of the streamwise fluctuating velocity grew as the flow evolved downstream and was approximately $0.3H_j$ in the core of the wall jet flow at $x/H_j = 16$ as discussed in Gao and Ewing [1]. The measurements of the fluctuating pressure reported here were compared to measurements for a jet exiting a second channel with $W/H_j = 39$. The results were in good agreement. The spacing of the microphones in the second jet was larger (relative to the jet size), so only the results from the jet with $W/H_j = 19.5$ are presented here.

The fluctuating pressure on the wall below the attaching jet was measured using an array of 16 microphones that have flat responses for 20–5000 Hz. The microphones were mounted directly into blind cavities drilled from the bottom of the wall on a line 0.75 cm off the jet centerline. The microphones sensed the flow through a 1 mm diameter, 5 mm long pinhole drilled through the wall to the top of the cavity. The pinhole reduced the interference of the flow field by the microphones. The microphones were calibrated externally with a piston phone at 1000 Hz. The spectra of the fluctuating wall pressure and the phase of the cross spectra measured through the pinholes agreed with the results for an array of flush mounted microphones for frequencies up to 400 Hz [19] that was larger than the frequency of interest here. A reference microphone was used to measure the ambient noise in one experiment. The ambient noise was found to be less than 1% of the pressure measured below the flow for frequencies less than 400 Hz, so the noise was neglected. The microphones were positioned from $x/H_j = 0.5$ to 8 with a streamwise

spacing of $0.5H_j$ in one experiment, and from $x/H_j = 1$–16 with a streamwise spacing of H_j in a second experiment.

The velocity in the jet was measured using a cross hot-wire probe with an in-house anemometry system based on previous designs [20–22]. The sensors in the cross-wire probe had diameters of 5 μm and lengths of 1.5 mm. The probe was calibrated in a separate facility using a jet exiting a contoured nozzle that had a uniform outlet velocity profile. The response curves for the individual wires were fit with fourth-order polynomials, while the response of the cross-wire was fit using a modified cosine law [23]. The hot-wire probe was mounted on a computer controlled traverse that could be positioned with an accuracy less than 0.05 mm. Rectification, examined following [24], affected approximately 2.5% of the data points at the inner half-width of the attaching shear layer and essentially no data points at the locations used to examine the phase speed of the structures here.

The microphones and hot-wire anemometers outputs were sampled at a frequency of 2048 Hz for 150 independent blocks of 1024 data points when the hot-wire probe was positioned at 16 equally spaced locations above each microphone at $x/H_j \leq 8$ and 20 equally spaced locations above each microphone at $9 \leq x/H_j \leq 16$. The cross spectra of the fluctuating wall pressure between the different locations,

$$F_{pp}(x_1, x_2, f) = \frac{\overline{\hat{p}(x_1, f)\hat{p}^*(x_2, f)}}{T}, \tag{1}$$

were computed from 24 000 independent blocks of data taken during the measurements at all the different points in the flow field. Here, $\hat{p}(x_1, f)$ is the fluctuating wall pressure Fourier transformed in time, * is the complex conjugate and T is the length of each data block. The uncertainty in the magnitude of the cross-spectra was less than $\pm 0.7\%$ [25]. The uncertainty in the coherence γ_{pp} computed from these cross-spectra, estimated using $(1 - \gamma_{pp}^2)/(|\gamma_{pp}|\sqrt{N})$ [25] where N is the number of the independent data blocks, was less than $\pm 3\%$ when the coherence was larger than 0.2. The uncertainty in the phase angle determined from these cross-spectra, estimated using $\sqrt{1 - \gamma_{pp}^2}/(|\gamma_{pp}|\sqrt{2N})$ [25], was less than $\pm 2\%$ when the coherence was larger than 0.2.

The cross spectra of the fluctuating wall pressure and the fluctuating velocities, such as $F_{pv}(x_1, x_2, y_2, f)$ given by

$$F_{pv}(x_1, x_2, y_2, f) = \frac{\overline{\hat{p}(x_1, f)\hat{v}^*(x_2, y_2, f)}}{T}, \tag{2}$$

where $\hat{v}(x_2, y_2, f)$ is the fluctuating vertical velocity at the location (x_2, y_2) Fourier transformed in time, were computed by averaging the results from the 150 blocks measured at each point. The uncertainty in the cross-spectra were 8%, while the uncertainties in the coherence and phase computed from these cross-spectra were 40% and 28% when the coherence was 0.2, and 12% and 9% when the coherence was 0.5.

3. Results and discussions

The mean velocity field in the offset jet with $H_s/H_j = 1$ and the rms fluctuating pressure on the wall below the jet are shown in Figure 2. The offset jet curved toward the wall attaching to the wall at $X_r = 4.7H_j$ (determined using a surface oil flow visualization technique [1]) before developing into a wall jet flow. The development of the mean flow for this jet has been divided into

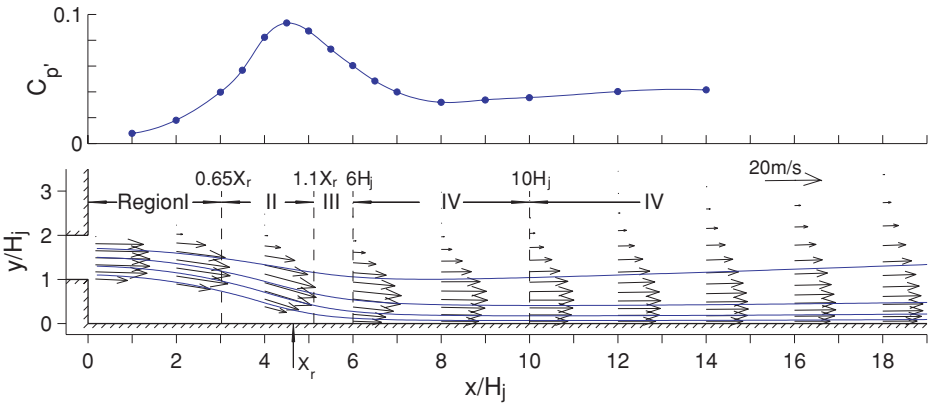

Figure 2. Distribution of the mean vectors and profile of the fluctuating wall pressure coefficient for the offset jet with $H_s/H_j = 1$ and $Re \approx 44\,000$.

five regions that were defined by Gao and Ewing [1] after considering jets with H_s/H_j from 0.2 to 1. The maximum mean velocity was approximately constant as the jet curved toward the wall in Region I ($x/X_r \leq 0.65$) before the maximum velocity decreased as the jet attached to the wall in Region II ($0.65 < x/X_r \leq 1.1$). The attaching jet recovered downstream of the reattachment point in Region III with an approximately constant maximum mean velocity before this velocity decreased as the flow transitioned to a wall jet flow in Region IV ($6 \lesssim x/H_j \lesssim 10$). The location of the maximum mean velocity moved toward wall in Region IV before moving away from the wall in Region V ($x/H_j \geq 10$), consistent with the results for a fully developed planar wall jet flow.

The magnitude of the rms fluctuating pressure reached a maximum slightly upstream of the reattachment point, before decreasing as the flow recovered downstream of the reattachment point consistent with other reattaching flows. The magnitude of the fluctuating pressure in the offset jet with $H_s/H_j = 1$ increased slowly beyond $x/H_j \approx 8$ similar to the results in a planar wall jet flow [1]. Gao and Ewing [1] found that the increase in the fluctuating pressure downstream of the reattaching point shifted downstream in terms of x/H_j as the offset distance increased indicating the change in the structures downstream of the reattachment point did not necessary correspond to the change in the mean flow field.

Typical spectra of fluctuating wall pressure and the fluctuating velocity components are shown in Figure 3. The spectra showed evidence of different characteristic frequencies. The frequency $fX_r/U_j \approx 1.4$ at $x/X_r = 0.43$ corresponds to the shear layer motions [1] and is evident in both the pressure- and vertical-velocity fluctuations. The characteristic frequency of the pressure- and vertical-velocity fluctuations decreased as the flow evolved downstream toward the reattachment point. The spectra downstream of the reattachment point showed evidence of lower-frequency fluctuations with $fH_j/U_j \approx 0.06$ as the wall jet structures became prominent [1]. This characteristic frequency at $x/H_j = 12$ is most evident in the fluctuating streamwise velocity nearer the wall and the fluctuating vertical velocity away from the wall indicating that the impact of these motions changed across the flow. The results at $x/H_j = 8$ showed evidence of fluctuations at both frequencies with the higher frequency most evident in the spectra of the vertical velocity near the wall, while the lower frequency was more evident in the fluctuations away from the wall indicating that both motions are present but in different parts of the flow as noted in [1].

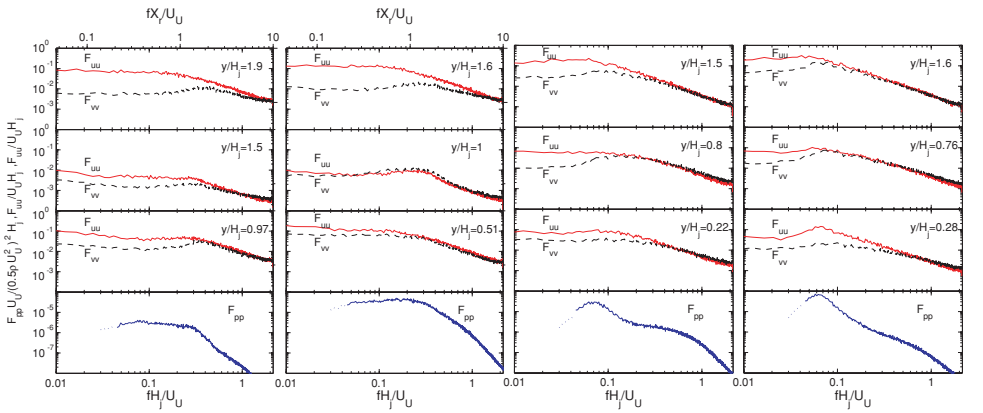

Figure 3. Spectra of the fluctuating wall pressure, fluctuating streamwise velocity, and fluctuating vertical velocity measured at $x/H_j = 2$, 4, 8 and 12 for an offset jet with $H_s/H_j = 1$ and $Re \approx 44\,000$.

3.1. *Propagation of the pressure fluctuations*

The coherence between the pressure fluctuations measured at different locations on the wall,

$$\gamma_{pp}(x_1, x_2, f) = \frac{|F_{pp}(x_1, x_2, f)|}{\sqrt{F_{pp}(x_1, x_1, f)F_{pp}(x_2, x_2, f)}}, \tag{3}$$

for reference points between $x_1/X_r = 0.11$ and 1.3 are shown in Figure 4. The pressure fluctuations had significant coherence over extended regions below this portion of the flow at three frequency ranges. The first with $fX_r/U_j > 0.6$ corresponds to the frequency of the structures in the attaching shear layer. The fluctuations have coherence over the largest region for frequencies of fX_r/U_j=1.2–1.4, the characteristic frequency near the separation point. The frequency range with large coherence increased significantly in Regions II and III where the structures attached to and traveled along to the wall to include motions with $0.6 < fX_r/U_j < 1.4$. The pressure spectra in Region II rolled off at $fX_r/U_j \approx 1$ near the center of this range.

The pressure fluctuations below the jet were also coherent for frequencies centered around $fX_r/U_j \approx 0.08$ similar to the frequency of the flapping motion observed in other reattaching flows [5,7,9,12,13]. This frequency was at the low end of the flat response range for the microphones so it was difficult to identify from the single point spectra. It was evident though in the coherence (and the measurements in the small jet where the dimensional values of the characteristic frequencies were higher). The coherence was poor near $x/X_r \approx 0.65$ and 1.1 suggesting that the fluctuations were not caused by a traveling motion. The coherence was also small beyond $x/X_r \gtrsim 1.5$ ($x/H_j \gtrsim 7$) indicating that the effect of the flapping motion did not extend into the wall jet region of the flow.

There was also coherence between the pressure fluctuations with $fX_r/U_j \approx 0.25$ (or $fH_j/U_j \approx 0.05$) near the jet outlet with those in Region IV downstream of the reattachment point. This frequency seemed to be associated with the wall jet motions downstream of the reattachment point ($x/X_r \gtrsim 1.1$ or $x/H_j \gtrsim 5$). The coherence of the fluctuations from the wall jet motions for reference points in Regions IV and V shown in Figure 5 were centered around $fH_j/U_j = 0.06$ (or $fX_r/U_j \approx 0.3$). The coherence between the pressure fluctuations at

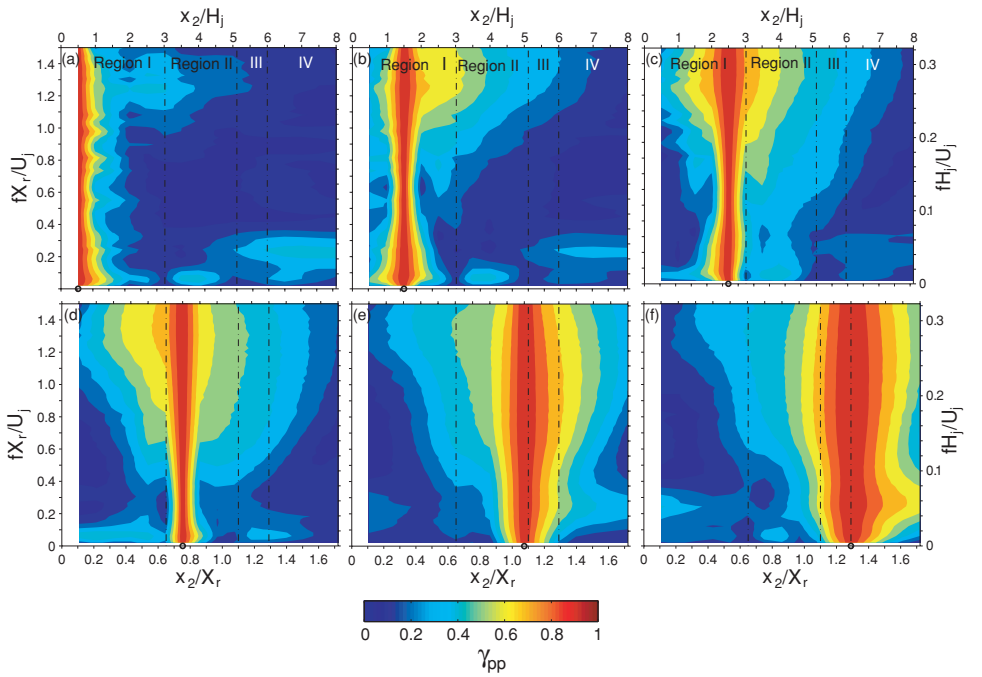

Figure 4. Coherence of the wall pressure fluctuations below the attaching offset jet for reference location at $x_1/X_r =$ (a) 0.11, (b) 0.32, (c) 0.54, (d) 0.75, (e) 1.08 and (f) 1.3.

the points in Regions IV and V and the point near the jet outlet were again centered around a slightly lower frequency. The link between these frequencies is not clear. There was not a large coherence over a significant region below the jet at a frequency of $0.2 \leq fX_r/U_j \leq 0.4$ except for the reference point at $x_1/X_r = 0.55$ suggesting the fluctuations at this frequency were caused by local motions.

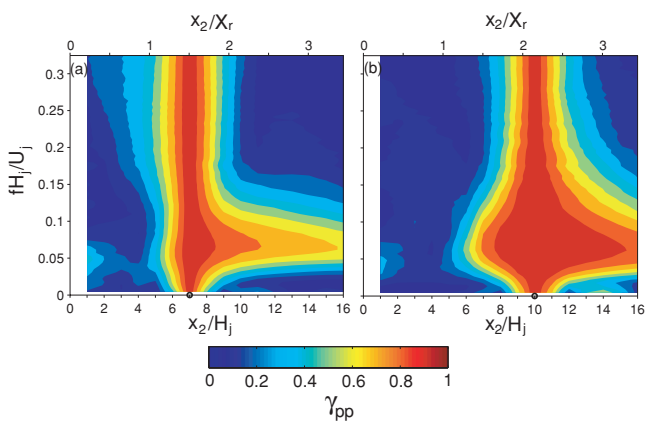

Figure 5. Coherence of the wall pressure fluctuations for reference locations at $x_1/H_j =$ (a) 7 and (b) 10.

Following Hudy et al. [8], the nature of the fluctuations at the different frequencies was characterized using the phase angle of the cross-spectra for different separation distances given by

$$\theta_{pp}(x_1, x_2, f) = \tan^{-1}\left(\frac{\text{img}(F_{pp}(x_1, x_2, f))}{\text{real}(F_{pp}(x_1, x_2, f))}\right). \tag{4}$$

The changes in the phase angle with downstream position for reference points between $x_1/X_r = 0.11$ and 1.3 (Regions I–III) are shown in Figure 6 and 7. The results for $fX_r/U_j < 0.6$ and $fX_r/U_j \geq 0.6$ have been separated into different figures and the results for different frequencies have been offset by 2π for clarity. The phase angles for the fluctuations with $fX_r/U_j \geq 0.6$ (that correspond to the shear layer motions) increased approximately linearly with downstream locations over much of the region indicating that the fluctuations propagate across the surface. The phase velocity of these fluctuations determined from the slope of the lines do vary with frequency as discussed later.

The results for the frequencies of $fX_r/U_j = 0.08$ and 0.16 show that the fluctuations in Region I are approximately π out of phase with the fluctuations in Region II, and 2π out of phase (or in phase) with the fluctuations in Regions III. Thus, the flapping motion caused the pressure fluctuations in Region II, where the jet attaches to the wall to be out of phase with the fluctuations in the other regions. This pattern was true for all of the measurement locations. The results also showed evidence of upstream propagation at these frequencies in Region I and downstream propagation in Regions II and III.

The results were more complicated for the frequencies of $fX_r/U_j = 0.2 - -0.4$ (or $fH_j/U_j \approx 0.04$–0.09). There seemed to be three sub-regions in Region I, I-a ($x/X_r \leq 0.2$), I-b ($0.2 < x/X_r \leq 0.4$) and I-c ($0.4 < x/X_r \leq 0.65$), and two sub-regions in Region II, II-a ($0.65 < x/X_r < 0.9$) and II-b ($0.9 < x/X_r < 1.1$). The phase angle for frequencies $fX_r/U_j \leq 0.3$ decreased with positive separations in the streamwise direction for sub-region I-b indicating the fluctuations with these frequencies propagated upstream in this sub-region, but increased with streamwise separation in Regions II-b and III indicating the fluctuations propagated downstream in these regions. The fluctuations at locations in Region I-c were in phase, while the fluctuations in Region II-a tended to be in phase though out of phase with those in Region I-c (and those in Region II-b). Thus, the upstream propagation of fluctuations was initiated below the attaching shear layer. For frequencies with $fX_r/U_j \geq 0.3$, the pressure fluctuations were in phase in region I-c for the lower frequencies, but showed evidence of downstream propagation throughout Regions II and III. The location where the downstream propagation was initially moved upstream as the frequency increased until it was near the start of region I-c for $fX_r/U_j = 0.6$.

The phase velocity of the fluctuations at the different frequencies in the different regions were computed from the slope of the phase angle $\theta_{pp}(x_1, x_2, f)$ following [8]; i.e.,

$$\frac{U_c}{U_j} = \frac{2\pi(fX_r/U_j)}{[\mathrm{d}\theta_{pp}(x_1, x_2, f)/\mathrm{d}x_2]X_r}, \tag{5}$$

where x_1 is the reference location in the region of interest and x_2 is the varying location in the same region. The phase velocities in the Regions I-b through III are shown in Figure 8(a), while the phase velocities of the motions downstream of the attachment point determined from a similar analysis for reference locations in Region IV and V are shown in Figure 8(b). The phase velocity in sub-region I-c and II-a were not computed in many cases becaus the fluctuations were approximately in phase indicating the fluctuations were not propagating. (The resulting velocity

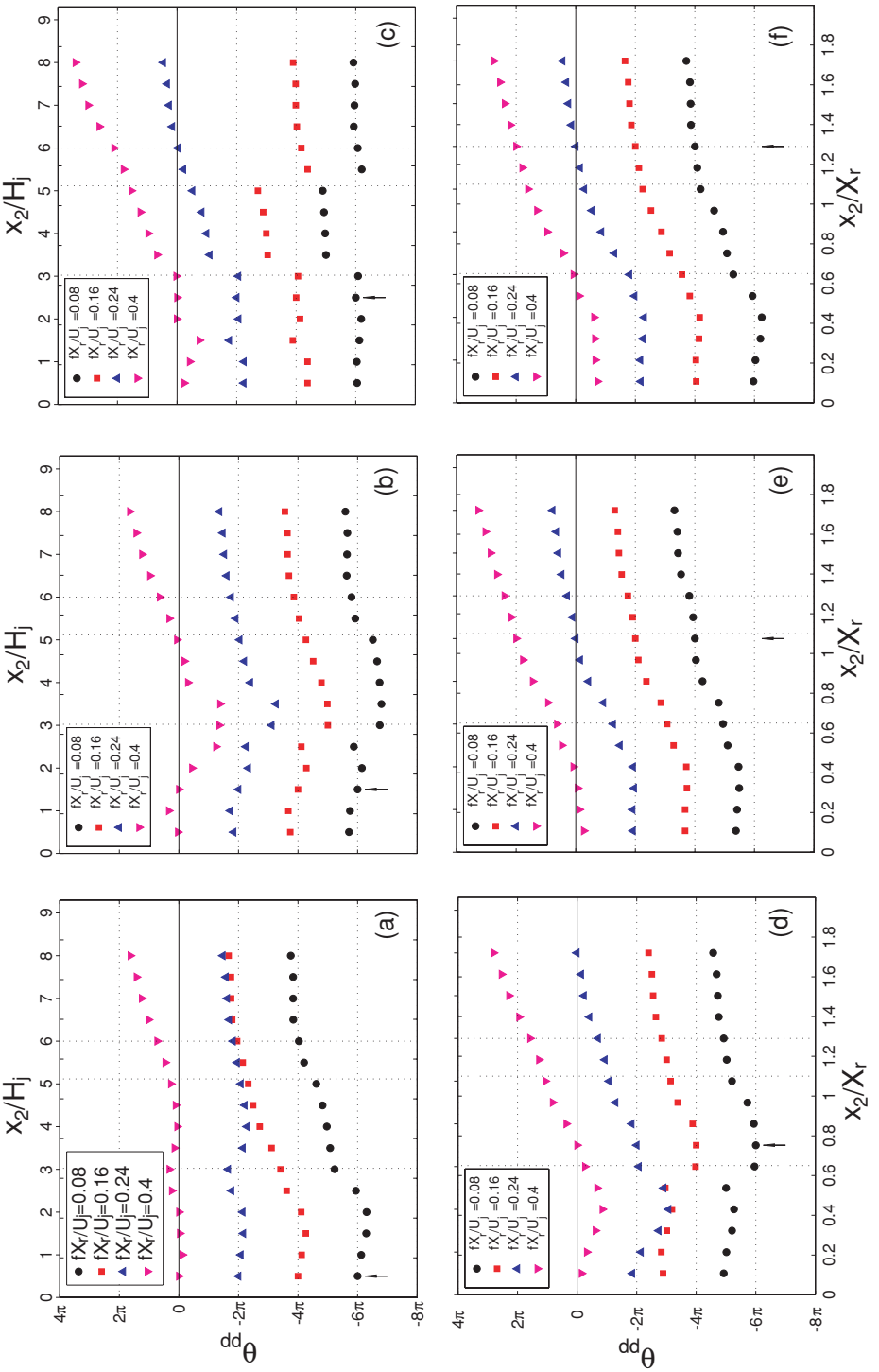

Figure 6. Phase angles of the pressure cross spectra for $fX_r/U_j < 0.6$ when $x_1/X_r =$ (a) 0.11, (b) 0.32, (c) 0.54, (d) 0.75, (e) 1.08 and (f) 1.3.

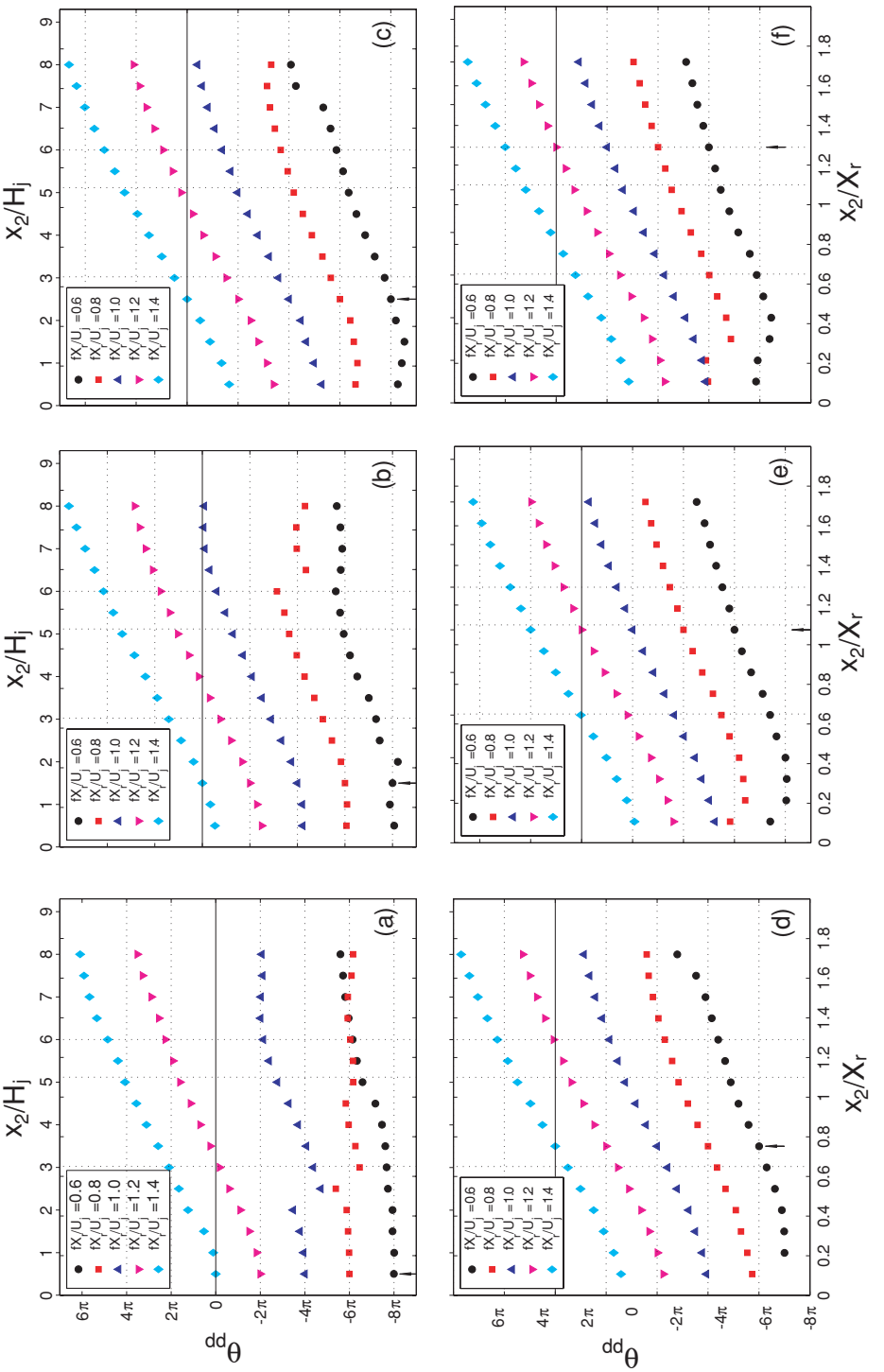

Figure 7. Phase angles of the cross spectra for $fX_r/U_j \geq 0.6$ when $x_1/X_r =$ (a) 0.11, (b) 0.32, (c) 0.54, (d) 0.75, (e) 1.08 and (f) 1.3.

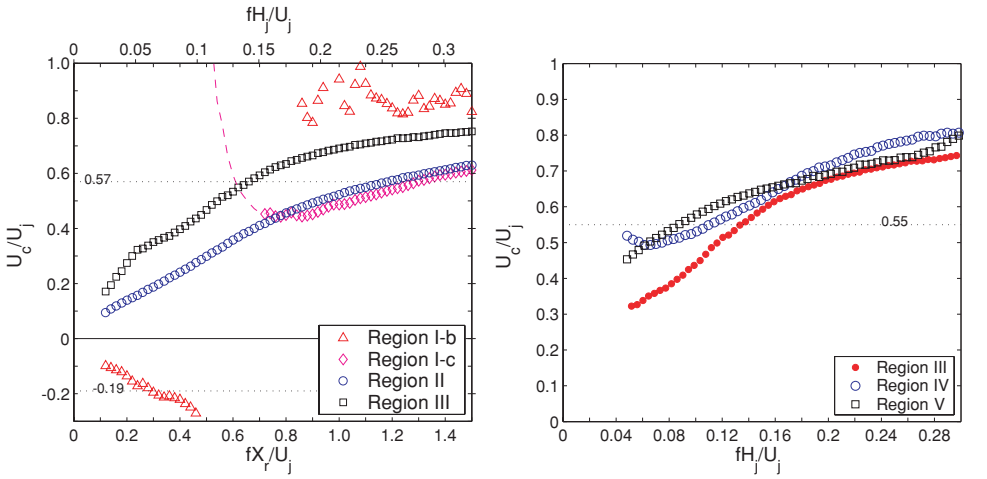

Figure 8. Phase velocity calculated using the phase angle of the pressure cross-spectra for (a) △ Region I-b ($0.2 \lesssim x_2/X_r \lesssim 0.4$), ◇ Region I-c ($0.4 \lesssim x_2/X_r \lesssim 0.6$), ○ Region II-b ($0.9 \lesssim x/X_r \lesssim 1.1$) or Region II and □ Region III ($1.1 \lesssim x/X_r \lesssim 1.3$) and (b) ● Region III, ○ Region IV and □ Region V for an offset jet with $H_s/H_j = 1.0$ and $Re \approx 44\,000$.

would be much larger than the jet velocity.) The results for Region II-a correspond to II-b when the fluctuations were not in phase so they have not been included as a separate curve.

The phase velocity in Regions I-b, II and III were approximately proportional to the frequency for $fX_r/U_j < 0.2$. This suggests there is a similar length scale structure being propagated at different speeds, where $l \sim U_c/f$. The length scale for the upstream motions were approximately X_r, while the length scale of the downstream motions was $0.75 - 1.5X_r$. Thus, the phase and phase velocity measurements suggest that the fluctuations in this frequency range are due to the unsteady dilatation and change in magnitude of the pressure distribution below the recirculation region due to the flapping motion. There is an approximately constant upstream phase velocity of $0.2U_j$ at frequencies of $0.3 < fX_r/U_j < 0.4$. This velocity agreed with the upstream velocity of $0.19U_j$ determined for the pressure correlation coefficients [1] indicating that the upstream propagation observed in the correlation measurements was not directly associated with the flapping motion. This frequency also corresponded to a peak observed in the pressure spectra in this region indicating the motions were dynamically significant.

The phase velocity of the motions with a frequency of $fX_r/U > 0.6$ varied throughout the attaching region decreasing between Regions I-b and I-c. The phase velocity of the motions increased after the reattachment point similar to the results from the flow over a backward facing step [7]. The phase velocity also varied with frequency as noted previously by Hudy et al. [8] for the flow over a fence. The propagation velocity determined from the correlation coefficient of the pressure in Region II was approximately $0.57U_j$ [1]. This agreed with the result for the fluctuations with $1.1 < fX_r/U_j < 1.3$ in sub-region I-c and Region II. The frequency was above the frequency where the pressure spectra roll off at the reattachment point, but did correspond to the frequency of the shear layer motions upstream of the reattachment point.

The phase velocity for the motions with the characteristic frequency of the wall jet structures ($fH_j/U_j \approx 0.06$) were approximately $0.5U_j$ in Regions IV and V. The average phase velocity in Regions IV and V determined from the correlation coefficient of the pressure in this region was approximately $0.55U_j$. The phase velocities of the high-frequency fluctuations $fH_j/U_j \geq 0.16$ or ($fX_r/U_j \gtrsim 0.8$) are similar in Regions III and IV. Thus, the propagation velocity of the fluctuations

associated with the shear layer motions are sustained downstream of the reattachment point and larger than the velocity of the wall jet motions.

3.2. *Fluctuating pressure-velocity measurements*

The relationship between the fluctuating pressure on the wall and the fluctuating velocity field was examined using the coherence between the pressure and the fluctuating velocity components given by

$$\gamma_{pu}(x_1, x, y, f) = \frac{|F_{pu}(x_1, x, y, f)|}{\sqrt{F_{pp}(x_1, x_1, f)F_{uu}(x, y, f)}} \tag{6}$$

and

$$\gamma_{pv}(x_1, x, y, f) = \frac{|F_{pv}(x_1, x, y, f)|}{\sqrt{F_{pp}(x_1, x_1, f)F_{vv}(x, y, f)}}, \tag{7}$$

and phase of the cross-spectra between the pressure and velocity. The results for a frequency of $fX_r/U_j = 0.08$ (that corresponds to the flapping motion) for $x_1/X_r = 0.43$ are shown in Figure 9. There are two regions where $\gamma_{pv} \geq 0.3$ on either side of the reattachment location. The phase shows that the wall pressure fluctuations at $x_1/X_r = 0.43$ were out of phase with the vertical velocity fluctuations at $x/X_r \lesssim 1$ and in phase with the fluctuations at $x/X_r \gtrsim 1$ indicating the jet was flapping vertically about a point near the reattachment location. The coherence between the streamwise fluctuating velocity and the pressure was largest near the reattachment point indicating the flapping affected the flow along the wall in this region.

The results for $fX_r/U_j = 1.0$ that corresponds to the shear layer motions are shown in Figure 10. The coherence between the fluctuating pressure on the wall at $x_1/X_r = 0.43$ and the fluctuating velocity was largest in the inner shear layer downstream of the measurement point of the pressure, and larger for the vertical velocity component. The pressure and the vertical velocity had regions in and out of phase along the shear layer consistent with motions propagating along the shear layer. There was coherence between the fluctuating pressure measured downstream of the reattachment point and the fluctuating velocity in this region, but this diminished downstream of the reattachment point indicating that the shear layer modes play a smaller role as the flow evolved downstream.

The results for a frequency of $fH_j/U_j = 0.06$ ($fX_r/U_j = 0.28$) that corresponds to the wall jet motions are shown in Figure 11. There was little coherence between the fluctuating pressure measured below the reattaching shear layer and the velocity in the flow at this frequency. There was coherence between the pressure downstream of the reattaching region and the velocity above the reattaching region indicating that the wall jet motions are formed upstream of the wall jet region (Regions IV or V). The coherence increased as the flow evolved downstream and the wall jet motions become more prominent. Interestingly, the coherence between the pressure and the vertical velocity component is largest near the wall and the outer edge of the jet, while the coherence between the pressure and streamwise velocity is largest in the center of the jet. Thus, it is not clear if these motions would make a large contribution to the Reynolds shear stress.

The coherence between the pressure and the velocity in the attaching jet was examined in more detail by repeating the measurements for 48 equally spaced locations on a line between $y/H_j = 1.25$ at $x/X_r = 0.01$ and $y/H_j = 0.75$ at $x/X_r = 1.5$ shown by the dotted line in Figure 10. The results for the pressure measured at different reference points are shown in Figure 12. The coherence between the fluctuating pressure and velocities was poor for the

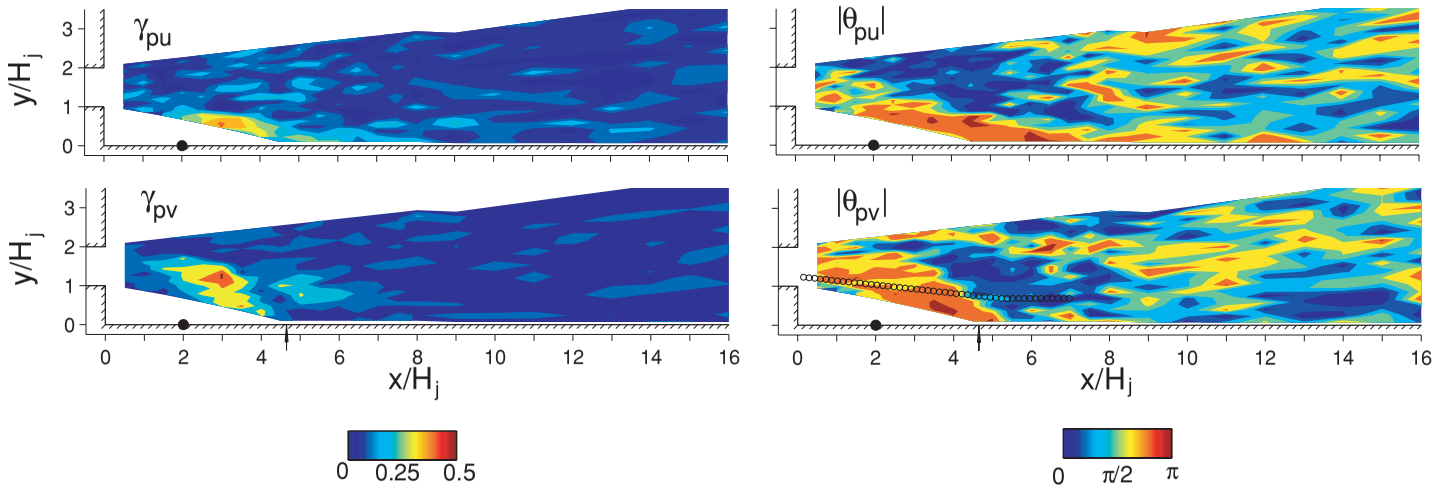

Figure 9. Distributions of the coherence and phase angle between the fluctuating wall pressure at $x/X_r = 0.43$ and the fluctuating streamwise and vertical velocities for the frequency $fX_r/U_j = 0.08$.

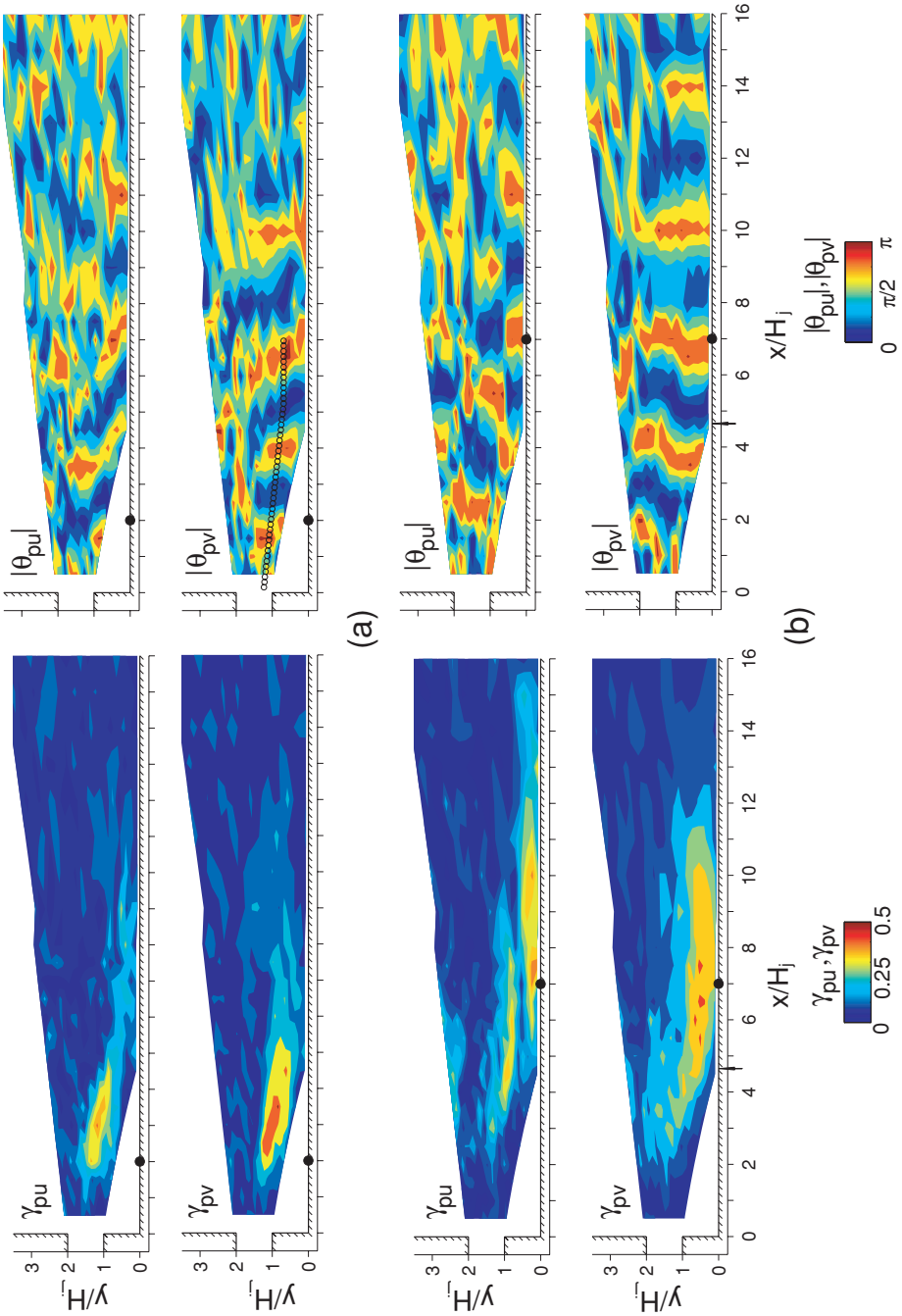

Figure 10. Distributions of the coherence and phase angle between the fluctuating wall pressure at (a) $x/X_r = 0.43$ and (b) $x_1/H_j = 7$ and the fluctuating streamwise and vertical velocities for the frequency $fX_r/U_j = 1$ or $fH_j/U_j = 0.2$.

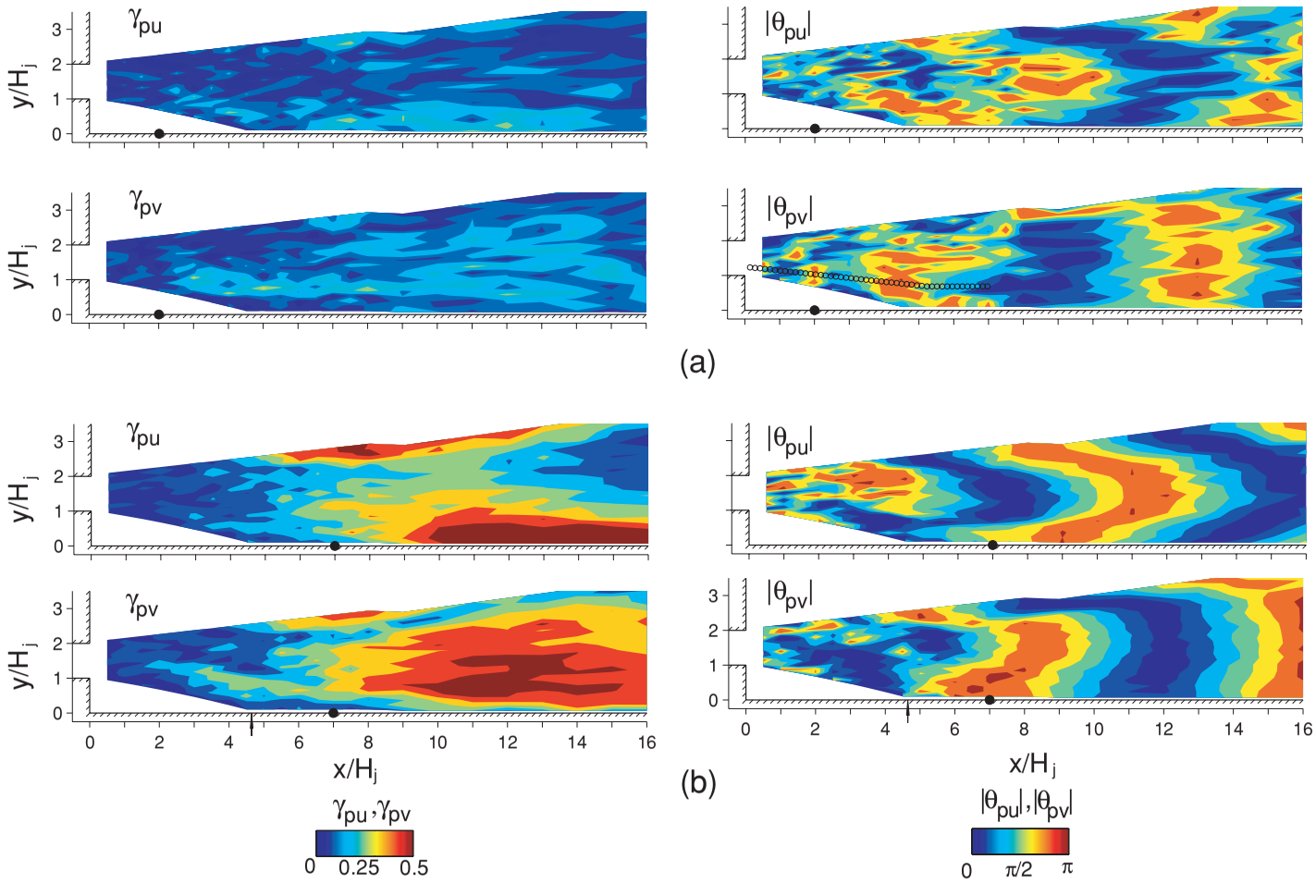

Figure 11. Distributions of the coherence and phase angle between the fluctuating wall pressure at (a) $x/X_r = 0.43$ and (b) $x_1/H_j = 7$ and the fluctuating streamwise and vertical velocities for the frequency $fX_r/U_j = 0.28$ or $fH_j/U_j = 0.06$.

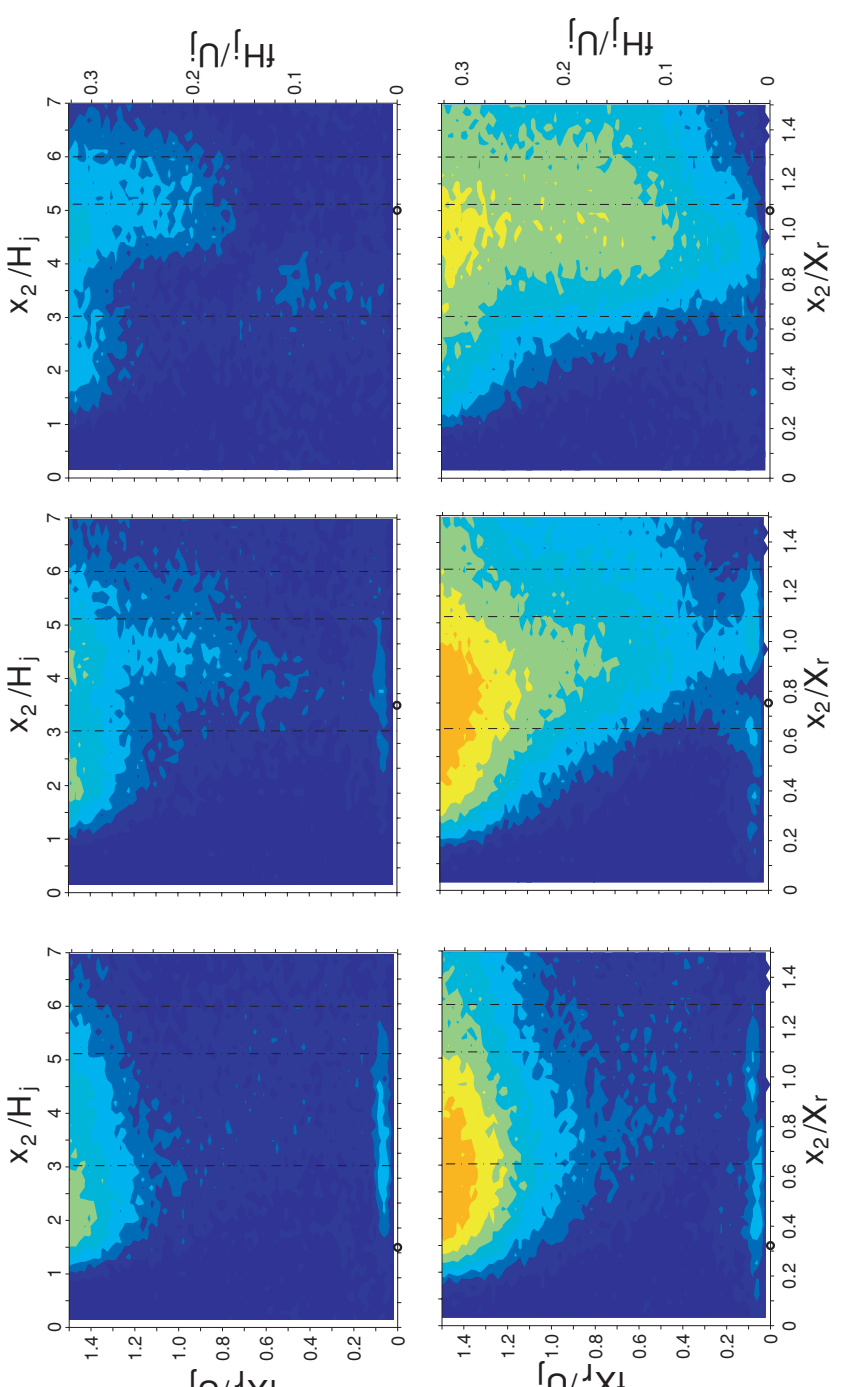

Figure 12. Distributions of the coherence between the fluctuating wall pressure and fluctuating velocities, γ_{pu} (top) and γ_{pv} (bottom) for the reference location at $x_1/X_r \approx 0.32$, 0.75 and 1.08 (from left to right).

frequencies of $0.1 < fX_r/U_j \leq 0.4$ for all locations indicating that the pressure fluctuations at frequencies of $0.2 < fX_r/U_j \leq 0.4$ below the attaching jet were not associated with the forward jet flow in Region I, but associated with the motions in the recirculating flow region below the jet. There was coherence between the pressure and the vertical velocity fields for $fX_r/U_j < 0.1$ except near $x/X_r \approx 0.82$ consistent with the results in Figure 9.

The coherence for the shear layer motions was initially largest for frequencies near $fX_r/U_j \approx 1.5$. This was higher than the frequency in the coherence from the pressure cross-spectra (Figure 4) because the largest contribution from the Poisson equation for the pressure is from the term linear in the gradient of the vertical fluctuating velocity. There was coherence between the fluctuating pressure with $1 < f/X_r/U_j < 1.5$ at all the points and the velocity in the flow from Regions I to III. The coherence for frequencies $0.6 < fX_r/U_j < 1$ was again large for Regions II and III ($x/X_r > 0.65$) where the structures attach to and travel along the wall, but small upstream of that location.

The phase velocities of the motions causing the velocity fluctuations in Regions II and III were examined by computing $\mathrm{d}\theta_{pv}/\mathrm{d}x$ from these measurements. The results are shown in Figure 13 with the results calculated from $\mathrm{d}\theta_{pp}/\mathrm{d}x$. The phase velocities determined from $\mathrm{d}\theta_{pv}/\mathrm{d}x$ in Regions II and III increased approximately linearly with frequency for $fX_r/U_j \lesssim 0.2$, indicating that the fluctuations at the different frequencies were caused by oscillations with a similar length scale. The length scale was approximately $1.6X_r$ in Region III, approximately twice the distance to the node in the flapping observed in the coherence γ_{pv} on this line, suggesting again this was caused by the unsteady dilatation of the recirculation region and change in the magnitude of the pressure distribution due to the flapping motion. The length is shorter for the results determined from the phase of the pressure cross-spectra because the distance to the nodes observed in that case were shorter.

The phase velocities determined from $\mathrm{d}\theta_{pv}/\mathrm{d}x$ differed from the results determined from $\mathrm{d}\theta_{pp}/\mathrm{d}x$ for the shear layer modes. The velocity determined from $\mathrm{d}\theta_{pv}/\mathrm{d}x$ were less frequency dependent for $0.6 < fX_r/U_j < 0.9$ in Regions II and III, and for $fX_r/U_j > 1.0$ in Region III. Thus, the phase velocity of the motions in the flow are likely not as frequency dependent as indicated by the wall pressure fluctuations. The acceleration of the motions downstream of the reattachment point determined from $\mathrm{d}\theta_{pv}/\mathrm{d}x$ was also smaller than from $\mathrm{d}\theta_{pp}/\mathrm{d}x$.

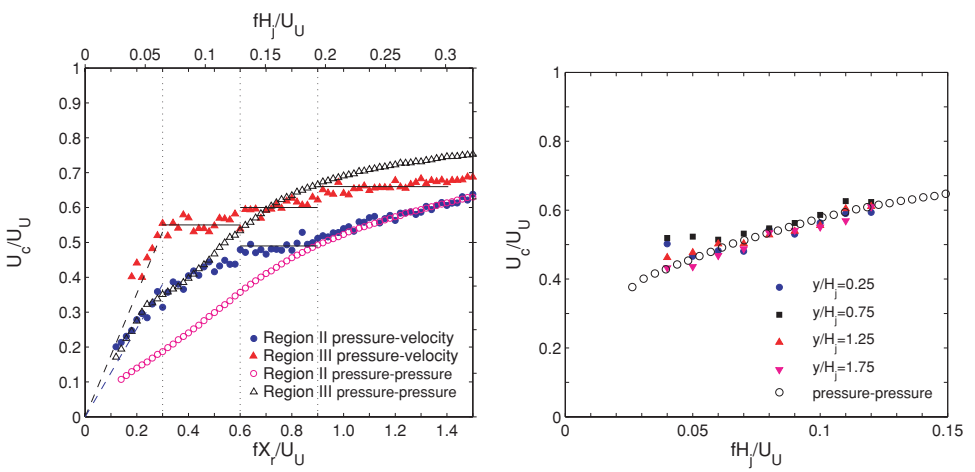

Figure 13. Propagation velocities computed using (open symbols) θ_{pv} and (solid symbols) computed using θ_{pp} in (a) Regions II and III and (b) Regions IV and V.

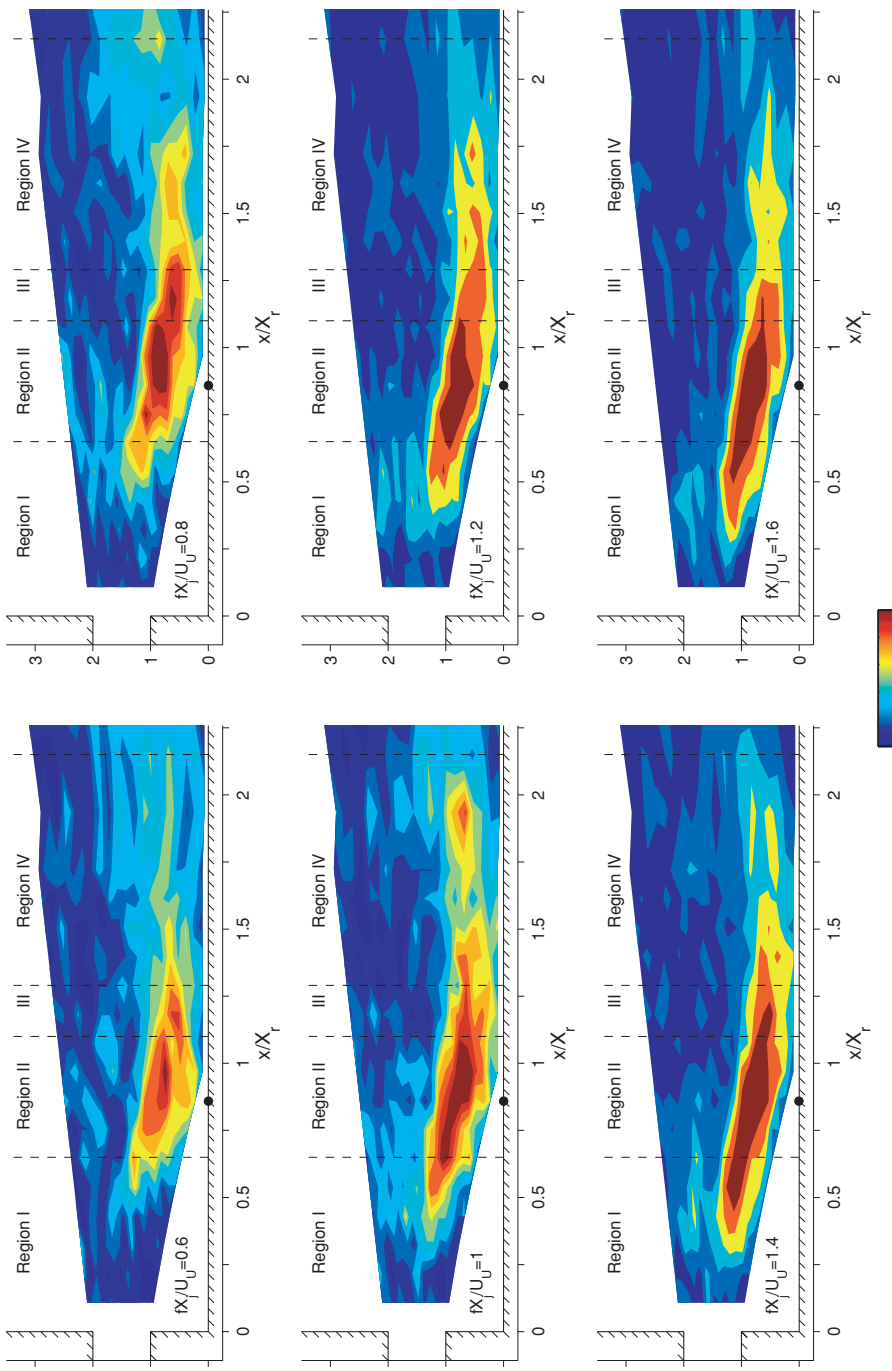

Figure 14. Distributions of the coherence between the fluctuating wall pressure and vertical fluctuating velocities, γ_{pv} for frequencies of $fX_r/U_j = 0.6$–1.6 with the reference location at $x_1/X_r \approx 0.86$.

There was evidence of three different velocities in the results from $d\theta_{pv}/dx$ in Region III in addition to the flapping at low frequencies. One was approximately $0.55U_j$ for $0.3 < fX_r/U_j < 0.6$ (or $0.07 < fH_j/U_j < 0.1$) that was associated with the structures that eventually form the wall jet structures. A second velocity of approximately $0.6\ U_j$ for $0.6 < fX_r/U_j < 0.9$ associated with the lower frequency shear layer motions formed in the reattachment region and a third velocity of approximately $0.67U_j$ for $1.0 < fX_r/U_j < 1.4$. The lower and higher velocities were not evident in the results from $d\theta_{pv}/dx$ in Region II, nor were any of these evident in the results from $d\theta_{pp}/dx$.

The difference in the motion with frequencies of $0.6 \leq fX_r/U_j \leq 0.9$ and those with higher frequencies is shown further in the coherence between fluctuating pressure and fluctuating vertical velocity (γ_{pv}) in Figure 14. The locations with large coherence extended throughout Regions I–III for the frequencies $fX_r/U_j \geq 1.0$. Thus, the higher-frequency motions seem to be associated with the shear layer structures passing along the wall relatively unaffected by the reattaching process since their frequency range corresponds to the motions upstream of the reattachment region and there is coherence throughout these regions. The coherence for $fX_r/U_j = 0.6$ and 0.8 can only be found in Regions II and III, where the shear layer interacts with the wall. The lower frequency range corresponds to structures with a lower phase velocity and larger characteristic length scale and thus, would seem to be shear layer motions more affected by the interaction with the wall. This could be due to the change in the trajectory of the shear layer toward the wall during the flapping of the shear layer, or these could be the 'wake-like' structures observed by [18,26]. The pressure fluctuations with constant upstream phase velocity (cf Figure 8(a)) occur at a subharmonic of this frequency range and thus, may be related to the these lower-frequency shear layer motions.

The results from similar measurements in the wall jet region are shown in Figure 13(b). The phase velocity determined from $d\theta_{pv}/dx$ agreed with the results from $d\theta_{pp}/dx$ at most frequencies. The former though showed less-frequency dependence for $fH_j/U_j = 0.05 - 0.07$ corresponding to the wall jet motions indicating that the variation of the phase velocity in $d\theta_{pp}/dx$ may not occur in the flow structures. The velocities from $d\theta_{pv}/dx$ at different heights agreed indicating there is a single wall jet structure.

4. Concluding remarks

An experimental investigation was performed to study the motions in an offset attaching planar jet with an offset distance of one jet height. Simultaneous measurements of the fluctuating wall pressure and the fluctuating velocities were performed. The coherence and phase angle of the cross-spectra of the measurements at different downstream points were considered in detail. The results indicated that there were four different motions associated with the attaching jet; a flapping motion affecting frequencies of $fX_r/U_j \lesssim 0.2$, a motion below the recirculating region with $0.3 \leq fX_r/U_j \leq 0.4$, shear layer motions with $1.0 \leq fX_r \leq 1.4$ and motions formed as the jet attached to the wall with frequencies of $0.6 \leq fX_r/U_j \leq 0.9$. Results from jets with different offset heights showed evidence that the relative contribution of the fluctuations with $0.6 \leq fX_r/U_j \leq 0.9$ and $1.0 \leq fX_r \leq 1.4$ to the fluctuating pressure change with offset height in the reattachment region further suggesting that these fluctuations are from different motions. Wall jet structures with frequencies of $0.05 \leq fH_j/U_j \leq 0.08$ ($0.24 \leq fX_r/U_j \leq 0.38$ for the jet with $H_s/H_j = 1$) also developed above the reattaching flow and became dominant as the flow-developed downstream. This rich frequency content in the flow suggests that attempts to estimate the velocity field from the fluctuating pressure or control the velocity field using the fluctuating pressure may require frequency or multi-time based methods [27–29] to fully capture the dynamics of the flow.

The wall pressure measurements showed evidence of upstream propagation near the separation point for the frequencies associated with the flapping motion and downstream propagation at this frequency as the shear layer attached to the wall. The phase velocity was proportional with the frequency over this range for both locations suggesting that the phase velocities are associated with the stretching or contraction of the pressure distribution below the jet as the recirculation region stretched or contracted due to the flapping. There was evidence of a constant upstream phase velocity similar to that observed in the correlation coefficient of the fluctuating pressure, but at a higher frequency of $0.3 < fX_r/U_j < 0.4$ that corresponded to a peak in the pressure spectra below the recirculation region. There was little coherence between the pressure at this frequency and the fluctuating velocities in the forward moving jet indicating these motions are associated with the recirculating flow.

The phase velocity of the shear layer motions determine from the phase of the cross-spectra between the fluctuating pressure and the fluctuating velocity showed significantly less-frequency dependence and less acceleration than the results determined from the pressure cross-spectra. There was also evidence of two different velocities for the motions with $fX_r/U_j > 0.6$ in and downstream of the reattaching region. The higher velocity corresponded to the frequency of the motions formed in Region I, while the lower velocity corresponded to the lower-frequency motions observed as the jet attaches to the wall. This lower velocity was not apparent in the results from the phase of the pressure cross-spectra. The measurements also showed that the wall jet motions developed above the attaching jet, though there was no evidence found of a connection between their formation and dynamics of the recirculation region. The phase velocity of the wall jet motions was slower than the shear layer motions as the flow initially recovered after attaching to the wall, and the velocity of both motions could be observed in the cross-spectra between pressure and the velocity. This was not the case for the results from the phase of the pressure cross-spectra. Thus, the phase velocities determined from cross-spectra of the pressure do not fully reflect the velocities of the motions in the flow.

Acknowledgment

The authors wish to acknowledge the support of Natural Sciences and Engineering Research Council of Canada.

References

[1] N. Gao and D. Ewing, *Experimental investigation of planar offset attaching jets with small offset distances*, Exp. Fluids 42 (2007), pp. 941–954.
[2] C. Chandrsuda and P. Bradshaw, *Turbulent structure of a reattaching mixing layer*, J. Fluid Mech. 110 (1981), pp. 171–194.
[3] L. Sigurdson, *The structure and control of a turbulent reattaching flow*, J. Fluid Mech. 298 (1995), pp. 139–165.
[4] A.J. Smits, *A visual study of separation bubble*, in *Flow Visualization* (2nd edn), W. Merzkirch, ed, (Washington, DC: Hemisphere), 1987, pp. 247–251.
[5] N. Cherry, R. Hillier, and M. Latour, *Unsteady measurements in a separated and reattaching flow*, J. Fluid Mech. 144 (1984), pp. 13–46.
[6] T. Farabee and M. Casarella, *Measurements of fluctuating wall pressure for separated/reattached boundary layer flows*, J. Vib. Acoust. Stress Reliab. Des. 108 (1986), pp. 301–307.
[7] A. Heenan and J. Morrison, *Passive control of pressure fluctuations generated by separated flow*, AIAA J. 36 (1998), pp. 1014–1022.
[8] L. Hudy, A. Naguib, and W. Humphreys, *Wall-pressure-array measurements beneath a separating/reattaching flow region*, Phys. Fluids 15 (2003), pp. 706–717.
[9] D. Driver, H. Seegmiller, and J. Marvin, *Time-dependent behavior of a reattaching shear layer*, AIAA J. 25 (1987), pp. 914–919.

[10] I. Lee and J. Sung, *Multiple-arrayed pressure measurement for investigation of the unsteady flow structure of a reattaching shear layer*, J. Fluid Mech. 463 (2002), pp. 377–402.
[11] P. Spazzini et al., *Unsteady behavior of back-facing step flow*, Exp. Fluids 30 (2001), pp. 551–561.
[12] M. Kiya and K. Sasaki, *Structure of a turbulent separation bubble*, J. Fluid Mech. 137 (1983), pp. 83–113.
[13] ———, *Structure of large-scale vortices and unsteady reverse flow in the reattaching zone of a turbulent separation bubble*, J. Fluid Mech. 154 (1985), pp. 463–491.
[14] H. Le, P. Moin, and J. Kim, *Direct numerical simulation of turbulent flow over a backwardfacing step*, J. Fluid Mech. 330 (1997), pp. 349–374.
[15] R. Simpson, *Turbulent boundary-layer separation*, Annu. Rev. Fluid Mech. 21 (1989), pp. 205–232.
[16] J. Eaton and J. Johnson, *A review of research on subsonic turbulent flow reattachment*, AIAA J. 19 (1981), pp. 1093–1100.
[17] R. Ruderich and H. Fernholz, *An experimental investigation of a turbulent shear flow with separation, reverse flow, and reattachment*, J. Fluid Mech. 163 (1986), pp. 283–322.
[18] L. Hudy, A. Naguib, and M. Humphreys, *Stochastic estimation of a separated flow field using wall pressure measurements*, Phys. Fluids 19 (2006) 024103.
[19] N. Gao, *Offset attaching planar jet with and with a co-flowing jet*, Ph.D. thesis, McMaster University, Hamilton, Canada, 2006.
[20] H. Sun, *Development of the three-dimensional wall jet*, Ph.D. thesis, McMaster University, Hamilton, Canada, 2002.
[21] A.E. Perry, *Hot-wire Anemometry* (Oxford: Clarendon), 1982.
[22] J. Citriniti, *Experimental investigation into the large structures of the axisymmetric mixing layer using the proper orthogonal decomposition*, Ph.D. thesis, State University of New York at Buffalo, Amherts, NY, 1996.
[23] H.H. Bruun, *Hot-wire Anemometry* (Oxford: Oxford University Press), 1995.
[24] N. Tutu and R. Chevray, *Cross-wire anemometry in high intensity turbulence*, J. Fluid Mech. 71 (1975), pp. 785–800.
[25] J.S. Bendat and A.G. Piersol, *Engineering Applications of Correlation and Spectral Analysis* (New York: John Wiley and Sons), 1993.
[26] D. Wee et al., *Self-sustained oscillations and vortex shedding in backward-facing step flows: Simulations and linear instability analysis*, Phys. Fluids 16 (2004), pp. 3361–3373.
[27] D. Ewing and J. Citriniti, *Examination of a LSE/POD complementary technique using single and multi-time information in the axisymmetric shear layer*. IUTAM Symp. on Simulation and Identification of Organized Structure in Flows, Lyngby, Denmark, 25–29 May 1997, J. Sorensen, E. J. Hopfinger, and N. Aubry, eds., Kluwer Academic Publishers.
[28] C. Tinney et al., *On spectral linear stochatistic estimation*, Exp. Fluids 41 (2006), pp. 763–775.
[29] L. Ukeiley et al., *Dynamic surface pressure based estimation for flow control*, IUTAM Symp. on Flow Control, 19–22 September, 2006, Imperial College, London.